Nonplanar Aromatic Compounds. 8.[1] Synthesis, Crystal Structures, and Aromaticity Investigations of the 1,*n*-Dioxa[*n*](2,7)pyrenophanes. How Does Bending Affect the Cyclic π-Electron Delocalization of the Pyrene System?

Graham J. Bodwell,*,[†] John N. Bridson,[†] Michal K. Cyrański,*,[§] Jason W. J. Kennedy,[†] Tadeusz M. Krygowski,[§] Michael R. Mannion,[†] and David O. Miller[†]

Department of Chemistry, Memorial University of Newfoundland, St. John's, NL, Canada, A1B 3X7, and Department of Chemistry, University of Warsaw, Pasteura 1, 02-093 Warsaw, Poland

gbodwell@mun.ca

Received September 16, 2002

A series of 1,*n*-dioxa[*n*](2,7)pyrenophanes (*n* = 7−12) with increasingly nonplanar pyrene moieties was synthesized by a 9−10 step sequence starting from 5-hydroxyisophthalic acid. The crystal structure of each member of this series was determined crystallographically. Several spectroscopic properties were found to vary with the extent of the nonplanarity of the pyrene unit. The way in which the distortion from planarity of the pyrene system influences its π-electron delocalization was investigated by using two quantitative descriptors of aromaticity based on geometry (HOMA) and magnetism (magnetic susceptibility and NICS). Both methods suggest that the aromaticity of the pyrene moiety is diminished only slightly upon increasing the bend angle θ from 0° to 109.2°.

Introduction

Aromaticity is a very important concept of "immense practical importance",[2b] as judged by the intense scrutiny it has received directly and in association with a very broad range of chemical investigations.[2]

Planarity is a structural feature that students of organic chemistry are taught at an early stage to associate with systems that are dubbed "aromatic". This geometrical arrangement normally corresponds to the bottom of an energy well and, sadly, this is often the limit of discussion at the introductory level. As with many other fundamentals of organic chemistry, such focus on the most energetically favorable geometry can lead to confusion and misconceptions at later stages. Thus the danger exists that the term "nonplanar aromatics" might be viewed as an oxymoron. In fact, a good number of systems containing nonplanar benzenoid rings are known and the overwhelming majority of these exhibit properties that are routinely linked to aromaticity.[3] Aromatic character clearly manifests itself at points on an energy surface other than the bottom of the well and the question becomes one of degree.

Within this context, considerable effort has been invested over the past few decades in attempting to understand how deviation from planarity might affect the π-electron delocalization commonly described by aromaticity.[4] [*n*]Paracyclophanes,[5a,6] [*n*]metacyclophanes,[5b,6] and other small cyclophanes[5c,6] have played a large role in such studies because they provide access to series of compounds that contain increasingly distorted benzene rings. A shortcoming of this work is that experimentally determined structural information is not available for most of the more distorted members of these series. As a result, it has been necessary to make recourse to calculations for structural information. Furthermore, work in

* To whom correspondence should be addressed. G.J.B.: fax (709)-737-3702. M.K.C: fax (+48) 22 822 28 92; e-mail chamis@chem. uw.edu.pl.
† Memorial University of Newfoundland.
§ University of Warsaw.

(1) Paper 7 in this series: Bodwell, G. J.; Bridson, J. N.; Chen, S.-L.; Li, J. *Eur. J. Org. Chem.* **2002**, 243−249.
(2) (a) Krygowski, T. M.; Cyrański, M.; Czarnocki, Z.; Häfelfinger, G.; Katritzky, A. R. *Tetrahedron* **2000**, *56*, 1783−1796. (b) *Chem. Rev.* **2001**, *101*, 1115−1566, thematic issue on aromaticity. (c) Schleyer, P. v. R.; Jiao, H. *Pure Appl. Chem.* **1996**, *68*, 209−218. (d) Minkin, V. I.; Glukhovtsev, M. N.; Simkin, B. Ya. *Aromaticity and Antiaromaticity—Electronic and Structural Aspects*; Wiley: New York, 1994. (e) Garratt, P. J. *Aromaticity*; McGraw-Hill: London, UK, 1971. (f) Cyrański, M. K.; Krygowski, T. M.; Katritzky, A. R.; Schleyer, P. v. R. *J. Org. Chem.* **2002**, *67*, 1333−1338. (g) Schleyer, P. v. R. *Chem. Rev.* **2001**, *101*, 1115−1117.
(3) See e.g.: Buhl, M.; Hirsch A. *Chem. Rev.* **2001**, *101*, 1153−1184.

(4) (a) Dijkstra, F.; van Lenthe, J. H. *Int. J. Quantum Chem.* **1999**, *74*, 213−221. (b) Grimme, S. *J. Am. Chem. Soc.* **1992**, *114*, 10542−10547. (c) Jenneskens, L. W.; Louwen, J. N.; de Wolf, W. H.; Bickel-haupt, F. *J. Phys. Org. Chem.* **1990**, *3*, 295−300.
(5) (a) Ma, B.; Sulzbach, H. M.; Remington, R. B.; Schaefer, H. F., III *J. Am. Chem. Soc.* **1995**, *117*, 8392−8400 and references therein. (b) van Eis, M. J.; de Wolf, W. H.; Bickelhaupt, F.; Boese, R. *J. Chem. Soc., Perkin Trans. 2* **2000**, 793−801. (c) Schuchmann, P.; Hafner, K. *Tetrahedron Lett.* **1995**, *36*, 2603−2606.
(6) (a) Smith, B. H. *Bridged Aromatic Compounds*; Academic Press: New York, 1964. (b) *Cyclophanes*; Keehn, P. M., Rosenfeld, S. M., Eds.; Academic Press: New York, 1983; Vols. 1 and 2. (c) *Top. Curr. Chem.* **1983**, *113*, 115. (d) Diederich, F. *Cyclophanes*; Royal Society of Chemistry: London, UK, 1991; (e) Vögtle, F. *Cyclophane Chemistry*; Wiley: New York, 1993. (f) *Top. Curr. Chem.* **1994**, *172*. (g) Kane, V. V.; de Wolf, W. H.; Bickelhaupt, F. *Tetrahedron* **1994**, *50*, 4575−4622. (h) Bodwell, G. J. *Angew. Chem., Int. Ed. Engl.* **1996**, *35*, 2085−2088. (i) de Meijere, A.; König, B. *Synlett* **1997**, 1221−1232. (j) Bodwell G. J. In *Organic Synthesis Highlights*; Schmalz, H. G., Ed.; Wiley-VCH: New York, 2000;,Vol. IV, pp 289−300. (k) Hopf, H. *Classics in Hydrocarbon Chemistry*; Wiley-VCH: Weinheim, Germany, 2000.

this area has been limited almost exclusively to systems that contain just a lone benzene ring. To the best of our knowledge, there has been no prior comprehensive, systematic experimental or theoretical study of the effect of distortion from planarity on the aromatic character of any polycyclic aromatic system.[7] In view of the strong current interest in nonplanar polycyclic aromatic molecules such as Buckybowls[8] and fullerenes,[3,9] the results of such a study could be particularly relevant, especially if X-ray crystal structures could be obtained.

Very recently we reported the syntheses of a variety of [*n*](2,7)pyrenophanes (**1b**,**c**, **2b**−**d**, **3**, **4**) in which the pyrene moiety is strongly distorted from planarity.[10] Pyrenophanes **1a** and **2a** have not yet been isolated. X-ray crystal structures were determined for most of these pyrenophanes and this opened the door to an investigation of the effect of bending on the aromaticity of the pyrene system, which manifests itself in the surfaces of several fullerenes (e.g. D_{5h}-C$_{70}$,[11] D_{5d}-C$_{80}$,[12] D_{6h}-C$_{84}$[13]) and Buckybowls (e.g. pinakene[14]). Having observed that the parent [*n*](2,7)pyrenophanes are the most dif-

ficult pyrenophanes to crystallize in a form suitable for X-ray crystallography,[10c] the 1,*n*-dioxa[*n*](2,7)pyrenophanes **1** were selected for the present investigation. We now report the synthesis of a series of 1,*n*-dioxa[*n*](2,7)-pyrenophanes **1b**−**g** and their X-ray crystal structures. The structural information serves as an excellent starting point for further analysis of the extent of changes of the cyclic π-electron delocalization in the pyrene system as it becomes increasingly nonplanar. This is done here through the application of quantitative measures of aromaticity: HOMA[15] (Harmonic Oscillator Model for Aromaticity, a geometry-based index) and NICS[16] (Nucleus-Independent Chemical Shift, a magnetism-based index). Of the many easily accessible quantitative definitions of aromaticity,[2d] it was anticipated[2f,g] that these two models would be the most efficient in accurately deducing the extent of stabilization due to the cyclic delocalization effect. Additionally, the values of magnetic susceptibility calculated for deformed pyrenes can also be used as an independent indicator of the extent of the changes of π-electron delocalization involved.[17]

1a n=4	**2a** n=6
1b n=5	**2b** n=7
1c n=6	**2c** n=8
1d n=7	**2d** n=9
1e n=8	
1f n=9	
1g n=10	

Discussion

Synthesis. Our approach to the [*n*](2,7)pyrenophane skeleton is based on the comprehensively studied valence isomerization between [2.2]metacyclophane-1,9-dienes **5** and 10b,10c-dihydropyrenes **6** (Scheme 1)[18] and the observation that when the internal substituents are hydrogen atoms (R = H), dehydrogenation of *trans*-**6** occurs readily to give pyrene **7**.[19] Presumably due to the length of the standard synthetic routes to [2.2]metacyclophane-1,9-dienes,[20] this valence isomerization/dehydrogenation (VID) protocol does not appear to have been utilized in any target oriented synthesis of a pyrene derivative prior to our involvement in this area. By introducing a third bridge of variable length between the 5 and 13 positions of the metacyclophanediene system **5**, we have been able to demonstrate that the parent

(7) Except for naphthalene, for which geometry-based investigations have been performed (see: (a) Krygowski, T. M. *Chem. Inf. Comput. Sci.* **1993**, *33*, 70−78. (b) Krygowski, T. M.; Cyrański, M. K. In *Theoretical and Computational Chemistry*; Parkanyi, C, Ed.; Elsevier: New York, 1998; Vol. 5) and fullerenes (see (c) Reference 3. (d) Krygowski, T. M.; Ciesielski, A. *J. Chem. Inf. Comput. Sci.* **1995**, *35*, 1001−1003).

(8) (a) Rabideau, P. W.; Abdourazek, A. H.; Folsom, H. E.; Marcinow, Z.; Sygula, A.; Sygula, R. *J. Am. Chem. Soc.* **1994**, *116*, 7891−7892. (b) Mehta, G.; Rao, H. S. P. *Tetrahedron* **1998**, *54*, 13325−13370. (c) Mehta, G.; Rao, H. S. P. In *Advances in Strain In Organic Chemistry*; Halton, B., Ed.; JAI: London, UK, 1997; Vol. 6, pp 139−187. (d) Rabideau, P. W.; Sygula, A. *Acc. Chem. Res.* **1996**, *29*, 235−242. (e) Siegel, J. S.; Seiders, T. J. *Chem. Br.* **1995**, 313−316. (f) Faust, R. *Angew. Chem., Int. Ed. Engl.* **1995**, *34*, 1424−1432. (g) Rabideau, P. W.; Sygula, A. In *Advances in Theoretically Interesting Molecules*; Thummel, R. P., Ed.; JAI: Greenwich, CT, 1995; Vol. 3, pp 1−36. (h) Scott, L. T.; Bronstein, H. E.; Preda, D. V.; Ansems, R. B. M.; Bratcher, M. S.; Hagen, S. *Atual. Fis.-Quim. Org.* **1999**, *11*, 138−150. (i) Scott, L. T.; Bronstein, H. E.; Preda, D. V.; Ansems, R. B. M.; Bratcher, M. S.; Hagen, S. *Pure Appl. Chem.* **1999**, *71*, 209−219. (j) Reisch, H. A.; Bratcher, M. S.; Scott, L. T. *Org. Lett.* **2000**, 2, 1427−1430. (k) Seiders, T. J.; Baldridge, K. K.; Siegel, J. S. *J. Am. Chem. Soc.* **1996**, *118*, 2754−2755. (l) Seiders, J. T.; Elliott, E. L.; Grube, G. H.; Siegel, J. S. *J. Am. Chem. Soc.* **1999**, *121*, 7804−7813. (m) Sygula, A.; Rabideau, P. W. *J. Am. Chem. Soc.* **1999**, *121*, 7800−7803. (n) Rabideau, P. W.; Sygula, A. *J. Am. Chem. Soc.* **1998**, *120*, 12666−12667.

(9) (a) Kroto, H. W.; Heath, J. R.; O'Brien, S. C.; Curl, R. F.; Smalley, R. E. *Nature* **1985**, *318*, 162−163. (b) Krätschmer, W.; Lamb, L. D.; Fostiropoulos, K.; Huffman, D. R. *Nature* **1990**, *347*, 354−358. (c) Scrivens, W. A.; Bedworth, P. V.; Tour, J. M. *J. Am. Chem. Soc.* **1992**, *114*, 7917−7919. (d) Hirsch, A. *The Chemistry of the Fullerenes*; Thieme: New York, 1994.
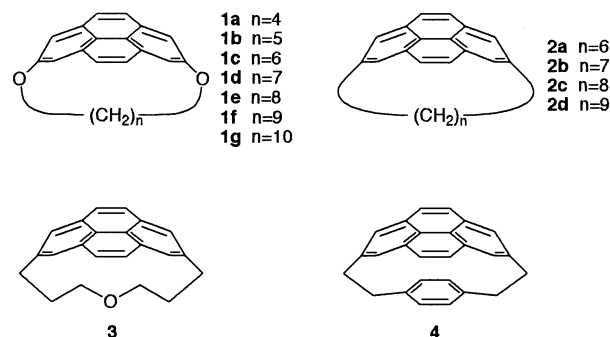
(10) (a) Bodwell, G. J.; Miller, D. O.; Vermeij, R. J. *Org. Lett.* **2001**, *3*, 2093−2096. (b) Bodwell, G. J.; Fleming, J. J.; Miller, D. O. *Tetrahedron* **2001**, *57*, 3577−3585. (c) Bodwell, G. J.; Fleming, J. J.; Mannion, M. R.; Miller, D. O. *J. Org. Chem.* **2000**, *65*, 5360−5370. (d) Bodwell, G. J.; Bridson, J. N.; Houghton, T. J.; Kennedy, J. W. J.; Mannion, M. R. *Chem. Eur. J.* **1999**, *5*, 1823−1827. (e) Bodwell, G. J.; Bridson, J. N.; Houghton, T. J.; Kennedy, J. W. J.; Mannion, M. R. *Angew. Chem., Int. Ed. Engl.* **1996**, *35*, 1320−1321.

(11) (a) Nikolaev, A. V.; Dennis, T. J. S.; Prassides, K.; Soper, A. K. *Chem. Phys. Lett.* **1994**, *223*, 143−148. (b) van Smaalen, S.; Petricek, V.; de Boer, J. L.; Dusek, M.; Verheijen, M. A.; Meijer, G. *Chem. Phys. Lett.* **1994**, *223*, 323−328. (c) Balch, A. L.; Catalano, V. J.; Lee, J. W.; Olmstead, M. M.; Parkin, S. R. *J. Am. Chem. Soc.* **1991**, *113*, 8953−8955. (d) Bürgi, H. B.; Venugopalan, P.; Schwarzenbach, D.; Diederich, F.; Thilgen, C. *Helv. Chim. Acta* **1993**, *76*, 2155−2159.

(12) Wang, C.-R.; Sugai, T.; Kai, T.; Tomiyama, T.; Shinohara, H. *J. Chem. Soc., Chem. Commun.* **2000**, 557−558.

(13) (a) Negri, F.; Orlandi, G.; Zerbetto, F. *J. Am. Chem. Soc.* **1991**, *113*, 6037−6040. (b) Manolopoulos, D. E.; Fowler, P. W. *J. Chem. Phys.* **1992**, *96*, 7603−7614. (c) Avent, A. G.; Dubois, D.; Pénicaud, A.; Taylor, R. *J. Chem. Soc., Perkin Trans. 2* **1997**, 1907−1910. (d) Cioslowski, J.; Rao, N.; Moncrieff, D. *J. Am. Chem. Soc.* **2000**, *122*, 8265−8270.

(14) Jemmis, E. V.; Sastry, G. N.; Mehta, G. *J. Chem. Soc., Perkin Trans. 2* **1994**, 437−441.

(15) (a) Krygowski, T. M.; Cyrański, M. *Tetrahedron* **1996**, *52*, 1713−1722. (b) Krygowski, T. M. *Chem. Inf. Comput. Sci.* **1993**, *33*, 70−78.

(16) (a) Schleyer, P. v. R.; Maerker, C.; Dransfield, A.; Jiao, H.; Hommes, N. v. E. *J. Am. Chem. Soc.* **1996**, *118*, 6317−6318. (b) Subramanian, G.; Schleyer, P. v. R.; Jiao, H. *Angew. Chem., Int. Ed. Engl.* **1996**, *35*, 2638−2641.

(17) (a) Dauben, H. J.; Wilson, J. D.; Laity, J. L. *J. Am. Chem. Soc.*, **1968**, *90*, 811−813. (b) Krishnan, K.; Bannerjee, *Philos. Trans. R. Soc. London, Ser. A* **1935**, *234*, 265.

(18) (a) Mitchell, R. H. In *Advances in Theoretically Interesting Molecules*; Thummel, R. P., Ed.; JAI Press: London, UK, 1989; Vol. 1, pp 135−199. (b) Mitchell, R. H. *Eur. J. Org. Chem.* **1999**, 2695−2703.

(19) Mitchell, R. H.; Boekelheide, V. *J. Am. Chem. Soc.* **1970**, *92*, 3510−3512.

(20) Mitchell, R. H. *Heterocycles* **1978**, *11*, 563−586.

SCHEME 1. Pyrenes from Metacyclophanedienes
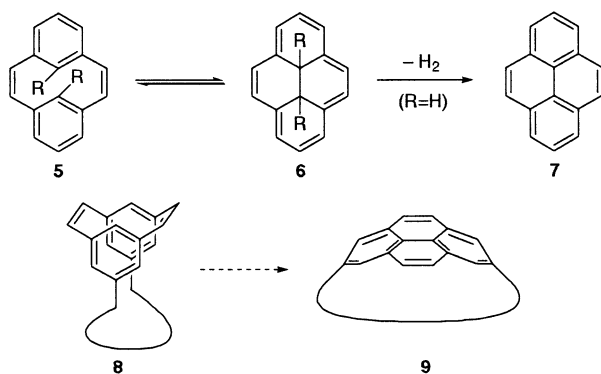
SCHEME 2[a]

transformation (**3** to **5**) is well suited to the synthesis of [*n*](2,7)pyrenophanes, i.e., **8** to **9**.

The syntheses of **1b** and **1c** have been previously reported[10d,e] and pyrenophanes **1d**−**g** were prepared along the same lines (Scheme 2). The synthesis of a potential precursor to **1a** is also described here. Tetraesters **11a,d**−**g** were prepared from diester **10** and could be isolated in good yield (64−89%). However, it proved to be more practical to subject the crude reaction mixtures to reduction with LiAlH$_4$ and then treat the resulting crude aluminum salts with HBr/H$_2$SO$_4$ to afford the tetrabromides **12a,d**−**g** in 42−65% overall yield from **10**. Formation of the dithiacyclophanes **13** (49−66%) was then achieved with Na$_2$S/Al$_2$O$_3$.[21] The yields of **13** are consistently within the normal range[10,21] and there does not appear to be a detrimental effect on the yield as the length of the tether increases from six to twelve atoms.

Twofold *S*-methylation of **13a,d**−**g** with (MeO)$_2$CHBF$_4$ (Borch reagent[22]), followed by Stevens rearrangement gave isomer mixtures **14a,d**−**g** (22−65%). These products were not characterized, but rather subjected to immediate bis(*S*-methylation) with Borch reagent. In contrast to the syntheses of **1b** and **1c**, subsequent reaction of the bis(methylsulfonium) salts derived from **14d**−**g** with *t*-BuOK did not afford the cyclophanedienes **15d**−**g**, but rather gave what appeared (by ^{1}H NMR analysis of the crude reaction mixtures) to be ca. 1:1 mixtures of pyrenophanes **1d**−**g** and dihydropyrenophanes **19d**−**g**. These compounds coeluted on silica under various conditions and were not separated. Instead the mixtures were treated with DDQ to give pyrenophanes **1d**−**g** (23−50%). The formation of **19d**−**g** can be explained by the initial formation of cyclophanedienes **15d**−**g**, which, due to the greater flexibility of the cyclophane moiety allowed by the longer tethers, valence isomerized under the conditions of their formation to give dihydropyrenophanes **16d**−**g**. Three consecutive [1,5]-H shifts lead to the generation of **19d**−**g**. Loss of H$_2$ from any of the dihydropyrenophanes **16**−**19d**−**g** results in the production of **1d**−**g**. With its much shorter tether, cyclophanediene **15a** formed in excellent yield (99%) and showed no inclination toward valence isomerization even when heated in mesitylene at reflux in the presence of DDQ.
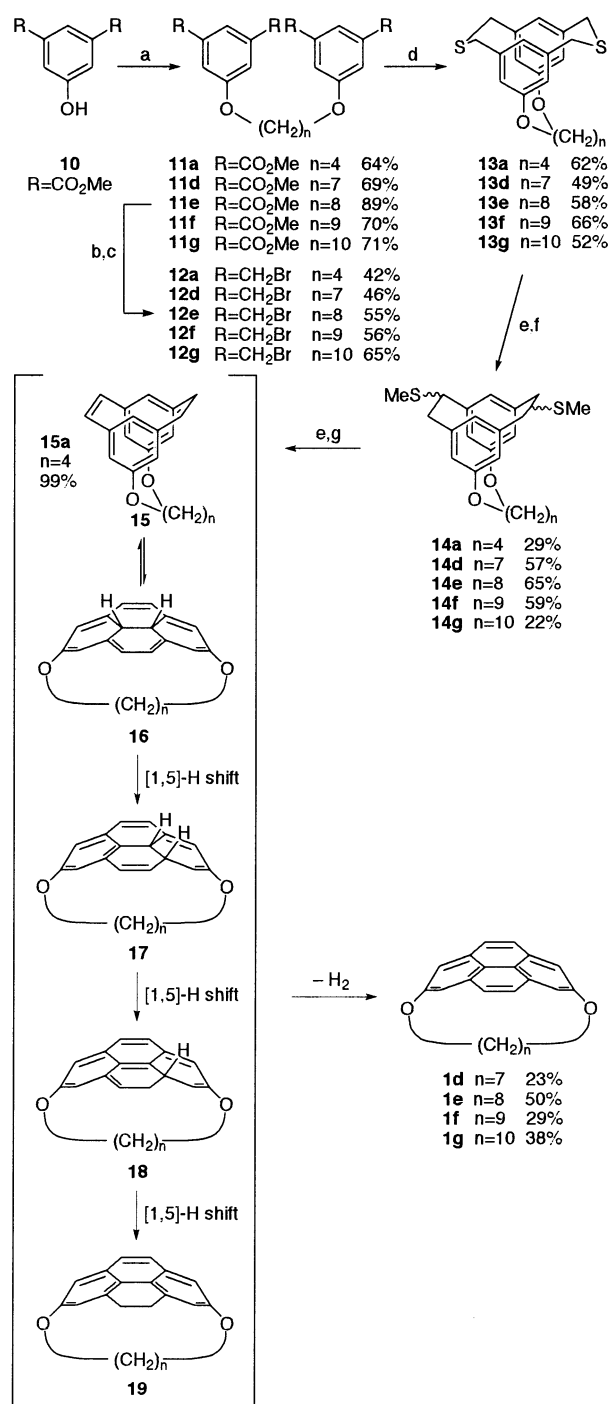
^{a} Reagents and conditions: (a) NaH, α,ω-dibromoalkane, TBAI, THF, 3 h, reflux; (b) LiAlH$_4$, THF, 14 h, rt; (c) 2:1 48% HBr(aq): H$_2$SO$_4$, 1 h, 70−90 °C; (d) Na$_2$S/Al$_2$O$_3$, 18% EtOH/CH$_2$Cl$_2$, 14 h, rt; (e) (MeO)$_2$CHBF$_4$, CH$_2$Cl$_2$, 3 h, rt; (f) *t*-BuOK, THF, 3 h, rt; (g) *t*-BuOK, 1:1 THF:*t*-BuOH, 6 h, rt, then (for **1d**−**g**) DDQ, benzene, 1−6 h, reflux.

X-ray Crystal Structures. The X-ray crystal structures of **1d**−**g** (Figure 1, Tables 1−3) were determined and this completed a series of 1,*n*-dioxa[*n*](2,7)pyrenophanes with bridge lengths ranging from 7 to 12 atoms (**1b**−**g**). Disorder in the bridge was observed for pyrenophanes **1e** and **1g**, which have even numbers of atoms

(21) Bodwell, G. J.; Houghton, T. J.; Koury, H. E.; Yarlagadda, B. *Synlett* **1995**, 751−752.

(22) For the original preparation of this reagent see: Borch, R. F. *J. Org. Chem.* **1969**, *34*, 627−629. Our procedure is given in the Supporting Information.
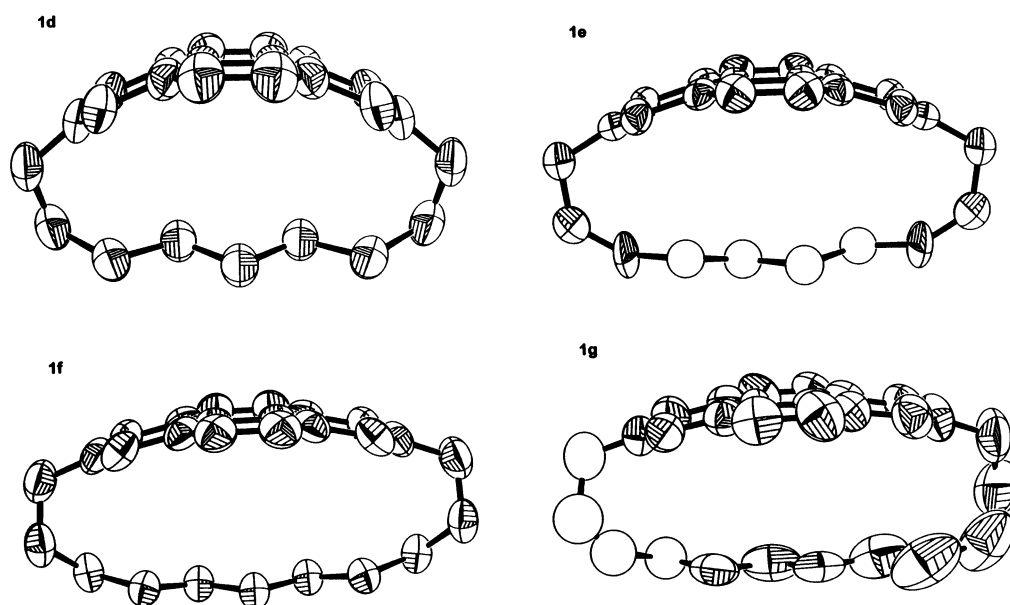
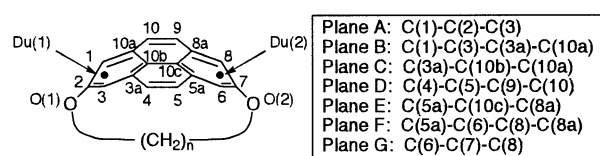**FIGURE 1.** ORTEP representations of **1d**−**g** in the crystal. Thermal ellipsoids are set at 50%.

TABLE 1. Crystallographic Data for 1d−g

	1d	1e	1f	1g
formula	$C_{23}H_{22}O_2$	$C_{24}H_{24}O_2$	$C_{25}H_{26}O_2$	$C_{26}H_{28}O_2$
M	330.43	344.45	358.48	372.51
cryst syst	orthorhombic	orthorhombic	orthorhombic	monoclinic
space group	Pnma	Cmcm	Pnma	Cc
cryst color	colorless	colorless	colorless	colorless
temp (K)	299	299	299	299
a (Å)	9.081(1)	17.661(3)	9.122(7)	23.490(2)
b (Å)	16.938(1)	11.144(2)	18.536(6)	7.445(2)
c (Å)	11.191(1)	9.120(3)	11.207(7)	13.692(1)
β (deg)				120.093(5)
V (Å³)	1721.4(3)	1795(1)	1895(3)	2071.6(4)
Z	4	4	4	4
D_{calc} (g cm^{-3})	1.275	1.275	1.256	1.194
total no. of reflns	1507	923	1949	1731
no. of unique reflns (R_{int})				1683 (0.010)
no. of observations	888	377	664	1135
no. of variables	150	67	125	251
no. of reflns/parameters	5.92	5.63	5.31	4.52
R, R_w	0.043, 0.043	0.074, 0.062	0.046, 0.032	0.046, 0.042
GOF	2.47	2.63	1.50	3.64

in their bridges. In the case of **1e**, the disorder was the result of equal occupancies of two enantiomeric forms, only one shown in Figure 1. As for **1g**, the disorder was localized at one end of the bridge and appears to be a consequence of looseness in the bridge. Pyrenophane **1g** exhibited no crystallographic symmetry lying in the general position, whereas **1d**, **1e,** and **1f** lay on a symmetry element and hence the two halves were symmetry related.

The crystallographic data enabled us to perform an analysis of the effect of the length of the bridge on the structural features of the pyrene unit. The angles formed by adjacent planes of atoms[23] in the pyrene systems of **1b**−**g** (Table 2) provided a means of quantifying the degree of bend. The overall bend in the pyrene skeleton (θ)[10b] is defined by the angle formed by the planes A and

(23) Where a group of three atoms is used, a plane is necessarily defined. Where a group of four atoms is used, a least-squares plane was determined mathematically.

TABLE 2. Angles (deg) between Least-Squares Planes of Atoms in 1b−g

Plane A: C(1)-C(2)-C(3)
Plane B: C(1)-C(3)-C(3a)-C(10a)
Plane C: C(3a)-C(10b)-C(10a)
Plane D: C(4)-C(5)-C(9)-C(10)
Plane E: C(5a)-C(10c)-C(8a)
Plane F: C(5a)-C(6)-C(8)-C(8a)
Plane G: C(6)-C(7)-C(8)

	plane									
compd	AB	BC	CD	DE	EF	FG	avg	AG (θ)	θ calc	β (deg)
1a									130.4	
1b[a]	18.2	16.0	20.5	20.5	16.1	17.9	18.2	109.2	113.3	8.2, 8.7
1c[b]	16.3	13.2	16.1	14.8	13.1	14.3	14.6	87.8	94.9	8.8, 8.8
1d	13.1	9.9	13.5	13.5	9.9	13.1	12.2	72.9	77.3	4.6, 4.6
1e	11.5	8.4	9.0	9.0	8.4	11.5	9.6	57.7	61.2	1.3, 1.3
1f	7.5	5.9	6.6	6.6	5.9	7.5	6.7	39.9	42.2	1.9, 1.9
1g	6.6	7.9	3.7	5.3	3.5	7.9	5.8	34.6	31.1	6.3, 7.1

[a] Reference 10d. [b] Reference 10e.

TABLE 3. Bond Angles (deg) in the Bridges of 1b–g

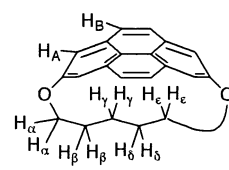| compd	C–O–C (avg)	O/C–C–C (range)	O/C–C–C (avg)
1b[a]	110.5	114.3–117.6	116.5
1c[b]	110.6	115.0–119.4	117.2
1d	111.8	115.4–120.3	118.3
1e	112.5	c	c
1f	113.7	112.9–116.1	114.6
1g	115.0	c	c

[a] Reference 10d. [b] Reference 10e. [c] Disorder in the bridge prevented determination of these bond angles.

G. The angle β, which is analogous to that used for [n]-paracyclophanes,[5a,6b,e] was determined by measuring the angles O(1)–C(2)–Du(1) and O(2)–C(7)–Du(2), where Du(1) is a dummy atom at the C(1)–C(3) centroid and Du(2) is a dummy atom at the C(6)–C(8) centroid (see Table 2).

For each of the pyrenophanes, the distortions from planarity are spread out quite evenly over the pyrene surface. As expected, the pyrene system becomes increasingly distorted from planarity as the length of the bridge decreases, as can been seen by the trends in the values of every interplane angle and θ (Table 2). The only anomalies occur with the highest homologue **1g** (BC and FG angles are larger than those of **1f**), which exhibits a less symmetric pattern of bend angles than the other pyrenophanes. This may be a consequence of the dynamic disorder that was observed at one end of the bridge. The β angles (Table 2) exhibit the expected trend, albeit a rather rough one, of diminishing with the degree of ranging from 8 to 9° for **1b** and **1c** down to 1–2° for **1e** and **1f**. Pyrenophane **1g** has anomalously large β angles (6.3°, 7.1°), which may well be artifacts originating from the disorder in the tether.

Although the principal focus of this study is the effect of the bridge on the pyrene unit, the effect of the pyrene unit on the bridge should not be overlooked. Since the strain in the pyrenophanes would be expected to be distributed over the entire molecular framework, it would seem reasonable to expect that the bridge should become increasingly strained as the pyrene unit becomes more distorted. Examination of models led to the prediction that the bond angles (C–O–C) about the terminal oxygen atoms of the bridge should become smaller as the pyrene system becomes more bent and that the remaining skeletal bond angles of the bridge (C–C–C) should become larger. In fact the C–O–C bond angles followed the expected trend (Table 3), as they decreased from an average of 115.0° in **1g** to an average of 110.5° in **1b**. By comparison, C_{aryl}–O–C_{alkyl} bond angles are normally in the range of 117 ± 0.7°.[24] Surprisingly, the O/C–C–C angles (angles around the remaining bridge atoms) did not follow the expected trend. In fact, the average C–C–C bond angles showed the opposite trend for the

(24) Based on 1183 molecular geometries of 885 systems (where *R is* <5% and the mean standard deviation of the bond length is <0.005 Å) retrieved from the Cambridge Structural Database. See also: (a) Allen, F. H.; Davies, J. E.; Galloy, J. J.; Johnson, O.; Kennard, O.; McRae Mitchell, E. M.; Mitchell, G. F.; Smith, J. M.; Watson, D. G. *J. Chem. Inf. Comput. Sci.* **1991**, *31*, 187–204. (b) Allen, F. H.; Bellard, S.; Brice, M. D.; Cartwright, B. A.; Doubleday: A.; Higgs, H.; Hummelink, T.; Hummelink-Peters, B. G.; Kennard, O.; Motherwell, W. D. S.; Rodgers, J. R.; Watson, D. G. *Acta Crystallogr.* **1979**, *B35*, 2331–2339. (c) For 1,3,5-trimethoxybenzene the $C_{(Phenyl)}$–O–CH₃ angles are 117.4, 117.4, and 118.3°. Howard, S. T.; Krygowski, T. M.; Główka, M. L. *Tetrahedron* **1996**, *52*, 11379–11384.

TABLE 4. ¹H Chemical Shifts (δ) for 1b–g and 21[a]

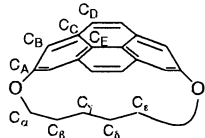| compd	H_A	H_B	H_α	H_β	H_γ	H_δ	H_ϵ
1b[b]	7.22	7.72	3.31	−0.04	−2.10		
	(0.63)	(0.24)	(1.00)	(1.45)			
1c[c]	7.44	7.84	3.59	0.10	−1.46		
	(0.41)	(0.14)	(0.72)	(1.31)			
1d	7.64	7.91	3.76	0.71	−1.89	−0.73	
	(0.21)	(0.05)	(0.55)	(0.70)			
1e	7.72	7.92	4.02	0.93	−1.17	−0.67	
	(0.13)	(0.04)	(0.29)	(0.48)			
1f	7.83	7.98	4.19	1.22	−0.27	−0.64	−1.04
	(0.02)	(−0.02)	(0.12)	(0.19)			
1g	7.85	7.96	4.31	1.41	−0.14	−0.14	−0.63
21	7.69	7.97	4.07				

[a] Bracketed numbers are the differences between a given chemical shift and the analogous shift for **1g**. [b] Reference 10d. [c] Reference 10e.

three lowest homologues, decreasing from 118.3° in **1d** to 117.2° in **1c** to 116.5° in **1b**. The higher homologue **1f** exhibited a smaller average angle of 114.6°, which is more in line with expectations. Unfortunately, data for the whole series could not be obtained due to disorder in the bridges of **1e** and **1g**. In any event, the counterintuitive trend for **1b–d** would suggest that the relative importance of the factors that determine the distribution of strain between the pyrene moiety and the bridge does not remain constant as the overall strain in the molecule varies.

Spectroscopic Properties. The signals in ¹H NMR spectra of **1b–g** and the comparison compound 2,7-dimethoxypyrene **21** were assigned by using standard 1D, 2D, and nOe experiments and are listed in Table 4. Several chemical shift trends with increasing bend in the pyrene unit were apparent. By using the least strained pyrenophane **1g** as a point of comparison, it can be seen that for the protons H_A, H_B, H_α, and H_β, there is a roughly linear correlation between $\Delta\delta$ ($\delta H_x - \delta H_{x(1g)}$) and the bend angle θ. In each case the trend is toward a higher field chemical shift with an increasing value of θ. The most pronounced effect is for the proton H_β, which varies over a range of 1.45 ppm. The ranges for H_α, H_A, and H_B are 1.00, 0.63, and 0.26 ppm, respectively. The remaining bridge protons, H_γ, H_δ, and H_ϵ, also show a tendency toward higher field with increasing θ, but the trends are not as well defined as for the other protons. This is likely a consequence of the positioning of these bridge protons deeper in the shielding zone of the pyrene nucleus, a region of high magnetic flux, than H_α and H_β.

It is particularly interesting to note that the trends for the aromatic protons of **1b–g** (higher field with increasing bend) are opposite to the situation for the [n]-paracylophanes (lower field with increasing bend).[25] Arguments based on diminished ring current[26] and rehybridization of the aromatic carbon atoms[27] with increasing bend would lead to the prediction of the

(25) Agarwal, A.; Barnes, J. A.; Fletcher, J. L.; McGlinchey, M. J.; Sayer, B. G. *Can. J. Chem.* **1977**, *55*, 2575–2581.

TABLE 5. ^{13}C Chemical Shifts (δ) for 1b–g and 21

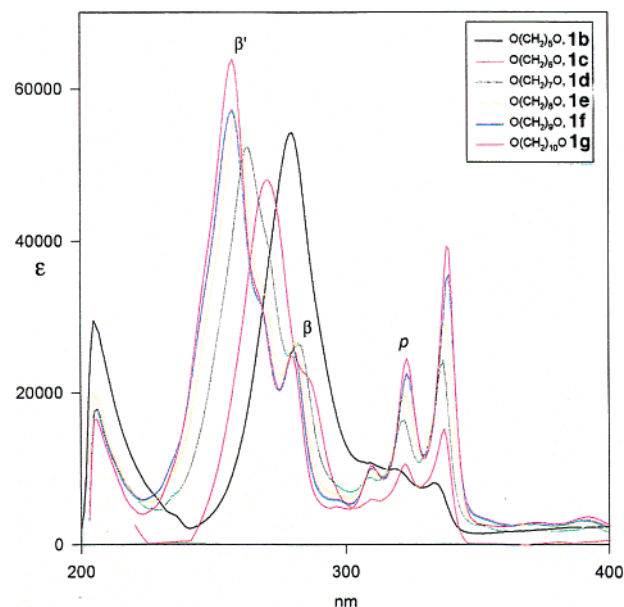| compd	C_A	C_B	C_C	C_D	C_E	C_α
1b[a]	152.0	123.1	133.4	126.7[c]	126.3[c]	76.3
1c[b]	153.6	123.2	132.7	126.9	127.4	77.7
1d	153.6	122.0	132.7	127.0	125.3	75.8
1e	154.8	121.0	132.3	127.1	123.6	76.3
1f	155.1	120.3	132.0	127.2	122.5	75.3
1g	156.9	118.7	131.9	127.2	121.8	74.2
21	157.1	110.6	131.5	127.5	120.1	55.8

[a] Reference 10d. [b] Reference 10e. [c] These signals could not be assigned unambiguously.

observed trends for the pyrenophanes. Why the observed trends for the two systems should oppose one another is unclear. It is, however, important to stress that bending does not involve dramatic changes of the chemical shifts of the protons attached to the pyrene moiety—the differences between the most bent pyrene derivative and the parent system are at most only 0.63 ppm. This suggests that the cyclic π-electron delocalization pattern is modified only moderately. Moreover, the extent of changes of proton shifts might imply that the π-electron structure of the outer rings is more influenced by strain as compared with the structure of the central ones.

^{13}C NMR data for the aromatic and OCH$_2$ carbons of **1b–g** are presented in Table 5. These were assigned by using standard 1D and 2D experiments. Most of the remaining bridge carbons could not be assigned due to the near degeneracy of their chemical shifts. It can be seen that C_D is essentially insensitive to changes in the degree of distortion from planarity of the pyrene system and that C_α shows no clear trend. Movement to lower field with an increase in bend of the pyrene unit can be seen for C_B (range = 4.5 ppm), C_C (range = 2.5 ppm), and C_E (range = 5.6 ppm). In the cases of C_B and C_E, the trend appears to taper off, or even reverse direction, as the bend angle reaches its maximum. Contrary to the other aromatic carbons, the bridgehead carbon atom (C_A) exhibits a trend to higher field with increasing bend (range = 4.9 ppm). We previously observed that C_E are the most pyramidalized carbon atoms in **1b**[10d] and **1c**,[10e] so it is perhaps not surprising that the widest range of chemical shifts is observed at this position. The paucity of ^{13}C NMR data for the [*n*]paracyclophanes[26] rules out a comparison to the trends observed for pyrenophanes **1b–g**.

$^1J_{C–H}$ values were measured for C_B, C_D, C_α, C_β, and C_γ of **1c**, **1d**, and **1e** (Table 6), but these did not show any clear trends. Furthermore, the percent s character calculated for these carbon atoms was normal, except at C_α, which exhibited greater s character than expected for an sp^3-hybridized carbon atom. Being at the periphery of the pyrene system, C_B and C_D would not be expected to

(26) (a) Allinger, N. L.; Freiberg, L. A.; Hermann, R. B.; Miller, M. A. *J. Am. Chem. Soc.* **1963**, *85*, 1171−1176. (b) Allinger, N. L.; Sprague, J. T.; Liljefors, T. *J. Am. Chem. Soc.* **1974**, *96*, 5100−5104. (c) Mori, N.; Takemura, T. *J. Chem. Soc., Perkin Trans. 2* **1978**, 1259−1262.
(27) Haddon, R. C. *Acc. Chem. Res.* **1988**, *21*, 243−249.

FIGURE 2. UV/vis spectra of **1b–g**.

TABLE 6. $^1J_{C–H}$ Values (Hz) and Percent s Character for Some Carbon Atoms of 1c–e

compd	C_B	C_D	C_α	C_β	C_γ
1c	161.0	162.7	146.3	128.0	125.3
	32.2%	32.5%	29.3%	25.6%	25.1%
1d	163.7	161.9	145.8	124.3	124.9
	32.7%	32.4%	29.2%	24.9%	25.0%
1e	160.5	161.1	146.4	123.8	128.8
	32.1%	32.2%	29.3%	24.8%	25.8%

experience significant pyramidalization/rehybridization. Thus the normal coupling constants and lack of trends for these carbons is understandable. On the other hand, bond angles in the bridge do appear to change with the length of the bridge (Table 3). It is therefore surprising to see that C_α, C_β, and C_γ show little or no variance with bridge length and that only C_α exhibits increased s character.

As for benzene, Clar has classified the absorption bands of pyrene according to their behavior with changes in temperature and solvent.[28] A strong absorption at 242 nm ($\epsilon = 8.84 \times 10^4$) is called the β' band and a second strong absorption at 273 nm ($\epsilon = 5.36 \times 10^4$) is called the β band. A series of three bands at 306, 320, and 336 nm ($\epsilon = 1.25 \times 10^4$, 3.23×10^4, 5.58×10^4) are termed the p bands. Finally, the α bands (352−372 nm) are very difficult to observe due to their very low extinction coefficients. The UV/vis spectra of less strained pyrenophanes (Figure 2) bear a strong resemblance to that of pyrene itself, with all of the bands having undergone a small red shift that would be expected to occur upon substitution at the 2 and 7 positions. As the bridge becomes shorter and the pyrene unit becomes more distorted, a number of systematic changes were observed. The β' band is markedly red shifted and the absorption becomes less intense. The β band experiences only a very slight red shift. The result of this is that the two bands

(28) Clar, E. *Spectrochim. Acta* **1950**, *4*, 116−121.

FIGURE 3. UV/vis spectra of **2b**–**d**.

FIGURE 4. Cyclic voltammograms of **1b**–**g**.

FIGURE 5. Cyclic voltammograms of **2b**–**d**.
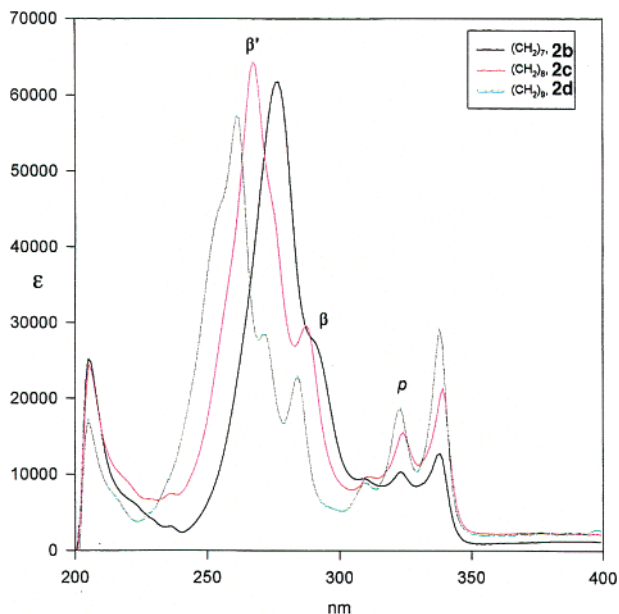
move closer together such that the β band is observed only as a shoulder on the β' band in the spectrum of **1c** and the two bands overlap completely in the spectrum of **1b**. The absorption maximum for this band (280 nm) is 23 nm red shifted from the β' band of **1g** (257 nm). The p bands do not appear to be significantly affected by the changes in the geometry of the pyrene system until the distortion becomes more pronounced, at which point there is a small blue shift. There is also a steady decrease in the intensity of the p bands with increasing distortion so that, in the spectrum of **1b**, they appear merely as poorly resolved humps. Similar trends are observed for the [n](2,7)pyrenophanes **2b**–**d** (Figure 3).

The electrochemistry of both pyrene[29] and D_{5h}-C$_{70}$,[30] which has a repeating pyrene unit around its equator, has been studied, so cyclic voltammetry was employed to ascertain whether fullerene-like behavior would begin to manifest itself as the degree of bend in the pyrene unit approached that of the pyrene substructures in fullerenes such as D_{5h}-C$_{70}$,[11] D_{5d}-C$_{80}$,[12] and D_{6h}-C$_{84}$.[13] Both the dioxapyrenophanes **1b**–**g** and the pyrenophanes **2b**–**d** show an irreversible first oxidation, which moves to lower potential as the bend in the pyrene system increases, i.e., oxidation occurs more easily as the aromatic nucleus becomes more distorted (Figures 4 and 5). This is consistent with the HOMO becoming higher in energy. A second oxidation wave is apparent, but there is no clear trend. By comparison, pyrene undergoes an irreversible oxidation at +1.54 V[29] and D_{5h}-C$_{70}$ undergoes an oxidation at +1.66 V, which is reversible under some conditions,[30b] but irreversible under others.[30c] Other than a marked increase in potential close to the switching potential (−2 V), no evidence of reduction is apparent in the negative scan region. On the other hand, it has been reported that

D_{5h}-C$_{70}$ is already reduced four times by the time a potential of −1.9 V has been reached.[30] On the whole, none of these results points to the emergence of fullerene-like behavior as the pyrene unit becomes more distorted. Comparisons to the [n]paracyclophanes were ruled out because there does not appear to be any reported study of their electrochemistry.

Aromaticity of the Pyrenophanes. To what extent can strain influence cyclic π-electron delocalization? The crystallographically determined molecular geometries of **1b**,[10d] **1c**,[10e] **1d**–**g**, pyrene **20**,[31] and [8](2,7)pyrenophane **2c**[10c] were used as the starting points for optimizations of the pyrene moieties. To cut off possible experimental errors and to eliminate the diversity of the data due to

(29) Peover, M. E.; White, B. S. *J. Electroanal. Chem.* **1967**, *13*, 93–99.

(30) (a) Echegoyen, L.; Echegoyen, L. E. *Acc. Chem. Res.* **1998**, *31*, 593–601. (b) Xie, Q.; Aria, F.; Echegoyen, L. *J. Am. Chem. Soc.* **1993**, *115*, 9818–9819. (c) DuBois, D.; Kadish, K. M.; Flanagan, S.; Wilson, L. J. *J. Am. Chem. Soc.* **1991**, *113*, 7773–7774.
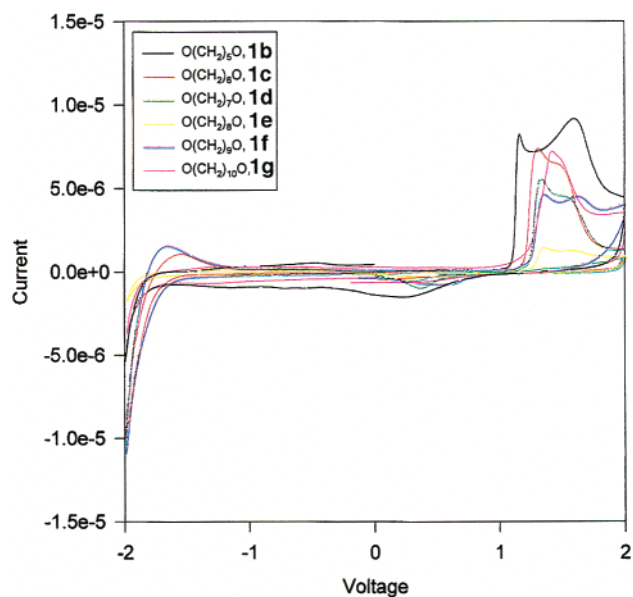
(31) (a) Kai, Y.; Hama, F.; Yasuoka, N.; Kasai, N. *Acta Crystallogr.* **1978**, *B34*, 1263–1270. (b) Frampton, C. S.; Knight, K. S.; Shankland, S.; Shankland, K. *J. Mol. Struct.* **2000**, *520*, 29–32.
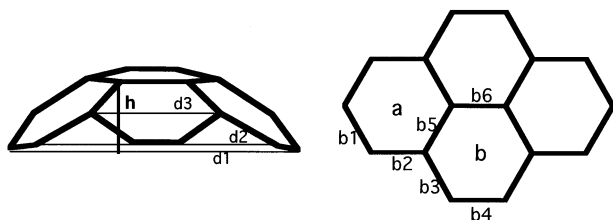
FIGURE 6. Distances and bond designations in the pyrene unit.

the influence of the oxygen neighborhood,[32] the pyrene systems were optimized with the bending parameters (d1, d2, and d3, see Figure 6) taken from X-ray experiments to maintain the proper shape of the moiety and implying C_{2v} and D_{2h} symmetry for pyrene derivatives and the parent system, respectively. The model geometries were optimized at the HF/6-31G** level of theory[33] and the resulting structures were used to calculate NICS values,[16a] which were computed at the HF/6-31G* level of theory, magnetic susceptibilities[17] at HF/6-311+G** using the CSGT method, and HOMA values.[15] NICS is a magnetism-based index, which is by definition[16a] the negative value of the absolute magnetic shielding in the center of the ring in question. A negative value of NICS is indicative of an aromatic system and a positive value points to an antiaromatic one. In principle, the model describes local aromaticity, although some attempts toward the global estimations have also been made.[16b,34] The exaltation of magnetic susceptibility, defined as a difference between the magnetic susceptibility of a given system and of a reference nonaromatic model one, is another well-known descriptor of global aromaticity.[2c,d,f,17] In the present work we compare the extent of changes of magnetic susceptibility with respect to pyrene. On the other hand, HOMA is a geometry-based index, which is described by eq 1

$$HOMA = 1 - \alpha(R_{opt} - R_{av})^2 - (\alpha/n)\sum(R_{av} - R_i)^2 = \\ 1 - EN - GEO \quad (1)$$

, where n is the number of bonds taken into the summation, α is an empirical constant fixed to give HOMA = 0 for a model nonaromatic system[15] and HOMA = 1 for the corresponding system in which all bonds are equal to the optimal value R_{opt}, which is assumed to be realized when full delocalization of the π electrons occurs (1.388 Å for CC bonds), R_{av} is the average bond , and R_i ($i = 1 - n$) are the individual bond lengths. The EN term describes lowering of aromaticity due to elongation of the bond lengths, whereas the GEO describes the lowering as a result of an increase of bond alternation. The advantage of HOMA is that it may be applied as a descriptor of both local and global aromaticity.[36] The models used here are easily accessible and have been proved as very efficient in the description of cyclic π-electron delocalization of many diverse π-electron systems.[2b,f,15,35,36,37]

As a result of optimizations for each pyrenophane **1b–g**, **2c**, and pyrene **20** the total energies of the systems, E_t, were calculated. These model values (E_t) varying by 210 kJ/mol are mostly affected by strain, and this is very well reflected in the good correlation with the bending parameter h (see Figure 6 –, the bending parameter h is almost perfectly equivalent to θ) with a correlation coefficient of $R = 0.962$. It is not an easy task to separate strain from the contribution due to the stabilization energy attributed to π-electron structure. Therefore the total energy values in fact are not very useful for the detailed analysis of the π-electron structure.

Table 7 contains values of HOMA, EN, GEO, and NICS for the terminal (a) and central (b) rings (Figure 6) of the pyrene systems, which are ordered in terms of decreasing distortion from planarity. The HOMA(a) values of the pyrenophanes span a range of 0.053 (0.078 if pyrene is included), whereas the corresponding HOMA-(b) values span a considerably larger range (0.146 for the pyrenophanes and 0.174 if pyrene is included). For both types of rings, the GEO term is dominant in determining the HOMA value, which indicates that changes in bond alternation are more significant than bond elongation as the degree of bend increases. The π-electron structure of the rings is not influenced much by strain despite the fact that the HOMA model may even slightly exaggerate the changes. This is due to the fact that, in strained systems, bond lengths calculated as the shortest distances between the nuclei are more adequately described by bond paths.[38] Moreover, the geometry-based indices describing π-electron effects may be much more strongly influenced by the σ-electron framework than the magnetic descriptors.[39]

Interestingly, in contrast to the trends observed for the HOMA values, the NICS values for the pyrenophanes vary substantially less in the central (b) rings (range = 1.05 ppm) than in the terminal (a) rings (range = 1.69 ppm). Both NICS(a) and NICS(b) values exhibit a general trend of decreasing aromaticity with increasing bend, and they both correlate well with the degree of bend (h) with correlation coefficients 0.939 and 0.885, respectively. Impressively good correlations exist between NICS(a) and NICS(b), NICS(a) and GEO(b), and NICS(b) and GEO-(b) (correlation coefficients $R = 0.985$, 0.950, and 0.934,

(32) (a) Hammett, L. P. *Physical Organic Chemistry*, 2nd ed.; McGraw-Hill: London, UK, 1970. (b) Chapman, N. B.; Shorter, J., Eds. *Correlation Analysis in Chemistry*, Plenum Press: London, UK, 1978.

(33) Frisch, M. J.; Trucks, G. W.; Schlegel, H. B.; Scuseria, G. E.; Robb, M. A.; Cheeseman, J. R.; Zakrzewski, V. G.; Montgomery, J. A., Jr.; Stratmann, R. E.; Burant, J. C.; Dapprich, S.; Millam, J. M.; Daniels, A. D.; Kudin, K. N.; Strain, M. C.; Farkas, O.; Tomasi, J.; Barone, V.; Cossi, M.; Cammi, R.; Mennucci, B.; Pomelli, C.; Adamo, C.; Clifford, S.; Ochterski, J.; Petersson, G. A.; Ayala, P. Y.; Cui, Q.; Morokuma, K.; Malick, D. K.; Rabuck, A. D.; Raghavachari, K.; Foresman, J. B.; Cioslowski, J.; Ortiz, J. V.; Stefanov, B. B.; Liu, G.; Liashenko, A.; Piskorz, P.; Komaromi, I.; Gomperts, R.; Martin, R. L.; Fox, D. J.; Keith, T.; Al-Laham, M. A.; Peng, C. Y.; Nanayakkara, A.; Gonzalez, C.; Challacombe, M.; Gill, P. M. W.; Johnson, B. G.; Chen, W.; Wong, M. W.; Andres, J. L.; Head-Gordon, M.; Replogle, E. S.; Pople, J. A. *Gaussian 98*, revision A.7; Gaussian, Inc.: Pittsburgh, PA, 1998.

(34) Schleyer, P. v. R.; Manoharan, M.; Jiao, H. J.; Stahl, F. *Org. Lett.* **2001**, *3*, 3643–3646.

(35) Patchkovskii, S.; Thiel, W. *J. Mol. Model.* **2000**, *6*, 67–75.

(36) Cyrański, M. K.; Krygowski, T. M.; Wisiorowski, M.; Hommes, v. E. N. J. R. *Angew. Chem., Int. Ed.* **1998**, *37*, 177–180.

(37) Krygowski, T. M.; Cyrański, M. In *Advances in Molecular Structure Research*; Hargittai, I., Hargittai, M., Eds.; JAI Press: London, UK, 1997; Vol. 3, pp 227–268.

(38) (a) Bader, R. F. W. *Atoms in Molecules: a Quantum Theory*; Oxford University Press: Oxford, UK, 1990. (b) Boese, R.; Blaser, D.; Billups, W. E.; Haley, M. M.; Maulitz, A. H.; Mohler, D. L.; Vollhardt, K. P. C. *Angew. Chem., Int. Ed. Engl.* **1994**, *33*, 313–317.

(39) (a) Krygowski, T. M.; Pindelska, E.; Cyrański, M. K.; Häfelinger, G. *Chem. Phys. Lett.* **2002**, *359*, 158–162. (b) Fowler, P. W.; Hevenith, R. W. A.; Jenneskens, L. W.; Soncini, A.; Steiner, E. *Chem. Commun.* **2001**, 2386–2387.

TABLE 7.   Aromaticity Indices for Compounds 1b−1g, 2c, and 20

	HOMA(a)	EN(a)	GEO(a)	NICS(a)	HOMA(b)	EN(b)	GEO(b)	NICS(b)
1b	0.929	0.001	0.070	−12.59	0.305	0.250	0.444	−3.77
1c	0.917	0.000	0.083	−13.21	0.392	0.214	0.393	−4.20
2c	0.906	0.000	0.094	−13.46	0.373	0.227	0.400	−4.25
1d	0.913	0.000	0.087	−13.63	0.451	0.183	0.366	−4.47
1e	0.886	0.000	0.114	−13.96	0.399	0.232	0.369	−4.69
1f	0.876	0.000	0.124	−14.27	0.422	0.222	0.356	−4.89
1g	0.884	0.000	0.116	−14.28	0.441	0.207	0.353	−4.82
20	0.962	0.014	0.034	−14.14	0.479	0.176	0.344	−4.63

TABLE 8.   Bond Lengths of Pyrene Moiety

system	b1	b2	b3	b4	b5	b6
1b	1.375	1.382	1.455	1.335	1.413	1.444
1c	1.373	1.380	1.450	1.336	1.414	1.437
2c	1.374	1.375	1.451	1.337	1.415	1.438
1d	1.372	1.379	1.447	1.336	1.414	1.430
1e	1.371	1.376	1.448	1.338	1.418	1.438
1f	1.369	1.377	1.446	1.338	1.419	1.436
1g	1.372	1.372	1.446	1.338	1.417	1.434
20	1.384	1.391	1.446	1.339	1.411	1.432

TABLE 9.   Correlation Coefficients between h and b1−b6

	h	b1	b2	b3	b4	b5
b1	−0.2456					
b2	−0.1383	0.8495				
b3	0.8793	0.0222	0.0387			
b4	−0.9604	0.2454	0.1579	−0.8196		
b5	−0.2223	−0.8397	−0.7916	−0.3245	0.2623	
b6	0.6179	−0.1673	−0.1330	0.8455	−0.4944	0.0849

respectively), indicating that despite different sensitivities of the rings to changes in the π-electron structure implied by strain, the aromaticity of one ring follows the changes in the other in a regular way. No other important correlation between the indices of the (a) and (b) rings was observed, which may suggest that the bond lengths in the two types of rings vary independently with bending. A Factor Analysis[40] (a statistical tool that decreases the number of variables and transforms them into orthogonal, i.e. independent vectors) of the bond lengths (b1−b6, Figure 6, Table 8) and the bending parameter h was performed and it showed that three factors describe 97.0% of the total variance. The first is loaded mostly with bonds constituting the (a) rings (48.8%), the second is loaded with b3, b4, and h (38.4%), and the third (9.8%) is loaded primarily with b6 and slightly with b3. A very similar picture emerged from a correlation analysis of the bond lengths (b1−b6, Figure 6) and the bending parameter h (Table 9). The bond types can be clustered into two groups, namely those of the (a) rings (b1, b2, and b5) and those of the (b) rings (b3, b4, and b6). As is evident from Table 9, correlations between bond lengths within clusters are good and those between bond lengths from different clusters are considerably worse. The bending parameter h correlates very well with b3 and b4 and to a lesser extent with b6, showing that these bond lengths regularly respond to changes in strain.

The global HOMA values and magnetic susceptibilities for the pyrene moieties of **1b−g**, **2c**, and **20** are presented

(40) Überla, K. *Faktorenanalyse*. Springer-Verlag: Berlin, Germany, 1977.

TABLE 10.   Bending Parameter (*h*), Energies, Global HOMA Values, and Magnetic Susceptibilities for 1b−g, 2c and 20[a]

	h [Å]	E_t [hartree]	rel E [kJ/mol]	HOMA	EN	GEO	magnetic suscept. [cgs·ppm]
1b	1.571	611.705797	210.2	0.593	0.042	0.366	−143.8
1c	1.248	611.735838	131.4	0.633	0.030	0.337	−148.3
2c	1.107	611.747755	100.1	0.618	0.028	0.354	−149.7
1d	0.994	611.753260	85.6	0.659	0.023	0.318	−150.8
1e	0.711	611.766989	49.6	0.631	0.027	0.342	−153.0
1f	0.298	611.778325	19.8	0.640	0.024	0.336	−154.5
1g	0.266	611.779988	15.4	0.648	0.020	0.333	−154.5
20	0.000	611.785868	0.0	0.696	0.051	0.253	−154.2

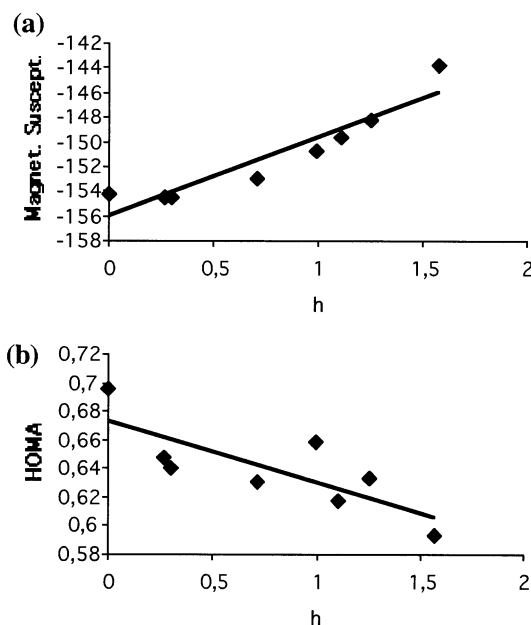[a] The experimental value for pyrene (**20**) is −154.9 (ref 17).

FIGURE 7. (a) Dependence between magnetic susceptibility and bending parameter h (correlation coefficient $R = 0.935$). (b) Dependence between HOMA and bending parameter h (correlation coefficient $R = 0.783$).

in Table 10, along with the bending parameter h and the total and relative energies. These provide the most important information concerning the changes in aromaticity as a function of bending, which is best illustrated by the plot of magnetic susceptibility against h, for which the correlation coefficient is 0.935 (Figure 7). HOMA correlated markedly worse, probably due to shortcomings mentioned above, but the correlation coefficient of 0.783 clearly indicates statistical significance[41] at the level of 0.05. This demonstrates that the extent of the cyclic π-electron delocalization of pyrene drops down in a regular way with an increase of strain over a broad

range of bend. However, the most important point is that the π-electron structure is almost untouched by the substantial increase in strain that accompanies the increase in bend in going from planar pyrene **20** to the most bent pyrenophane **1b**. HOMA changes by only 0.1 of a unit over this range, while the magnetic susceptibility varies by 10.4 units, which is even more striking when considering that the exaltation of magnetic susceptibility of planar pyrene is 57.3.[17] Moreover, insignificantly higher magnetic susceptibilities for slightly deviated pyrenes may be a sign that small deviations from planarity do not involve a dramatic drop in the π-electron delocalization pattern and weak intermolecular interactions may easily deform it, as is well-known in the case of benzene.[42]

Thus the answer to the question posed in the title is that despite substantial changes in the hybridization of carbon atoms involving changes in the σ-electron structure of pyrene, the aromaticity of the system decreases slightly and regularly with increasing bend. However the changes are not dramatic, even with the great increase in strain (approximately 210 kJ/mol). That aromaticity drops off with increasing departure from planarity is to be expected.[43] However, our results provide, for the first time, a clear indication of the extent to which aromaticity decreases with increasing nonplanarity.

Conclusions

The valence isomerization/dehydration approach was successfully applied to the synthesis of a series [*n*](2,7)-pyrenophanes **1b**−**g**, further establishing its scope. Several trends in the spectroscopic properties of the pyrenophanes were observed to accompany the increasing deviation from planarity of the pyrene system, but no evidence was found to suggest that increasing the degree of nonplanarity resulted in fullerene-like behavior of the pyrene moiety. HOMA, NICS, and magnetic susceptibility data all led to the conclusion that increasing the degree of bend in the pyrene system results in only a small, but regular, loss of aromaticity over a wide range of bend.

(41) Snedecor, G. W.; Cochran, W. G. *Statistical Methods*; The Iowa State University Press: Ames, IA, 1973; p 184.

(42) Jeffrey, G. A.; Ruble, J. R.; McMullan, R. K.; Pople, J. A. *Proc. R. Soc. (London)* **1987**, *A414*, 47.

(43) See for example: (a) Haddon, R. C. *Acc. Chem. Res.* **1988**, *21*, 243−249. (b) Haddon, R. C. *J. Am. Chem. Soc.* **1987**, *109*, 1676−1685. (c) Haddon, R. C. *J. Am. Chem. Soc.* **1990**, *112*, 3385−3389.

Experimental Section

Crystal Structure Determinations. Crystals suitable for X-ray diffraction experiments were obtained by crystallization from xylenes solutions. The measurements were performed at 299 ± 2 K on a Rigaku AFC6S diffractometer with graphite-monochromated Mo Kα (0.71073 Å) or Cu Kα (1.54056 Å) radiation. Data reduction and analysis were carried out with the TEXSAN or teXsan for Windows programs. The data were corrected for Lorentz and polarization effects. Absorption correction was applied where appropriate. The structures were solved by direct methods[44] and refined by using TEXSAN or teXsan for Windows.[45] The refinements were based on F for all reflections with $I > 2.00\sigma(I)$. The weighted R factor, wR, and all goodness-of-fit S values are based on F. All non-hydrogen atoms were refined anisotropically, except for **1g**, where some were refined isotropically. H-atoms were placed in calculated positions with isotropic thermal parameters set 20% greater than those of their bonding partners and were not refined, except for **1d**, in which they were optimized by positional refinement. The atomic scattering factors were taken from the International Tables.[46]

Cyclic Voltammetry. Cyclic voltammograms vs SSCE were obtained at a scan rate of 100 mV/s from Ar-degassed CN_3CN (distilled from CaH_2 directly prior to use) solutions containing tetraethylammonium perchlorate.

Supporting Information Available: Experimental procedures and characterization data for all new compounds and copies of ^1H and ^{13}C NMR spectra for all new compounds; absolute electronic energies, Cartesian coordinates, and magnetic susceptibilities for pyrene fragments of **1b**−**g**, **2c**, **20**; tabulated UV/Vis and CV data for **1b**−**g** and **2b**−**d**. This material is available free of charge via the Internet at http://pubs.acs.org. Crystallographic data for the structure have been deposited with the Cambridge Crystallographic Data Centre as supplementary material No. CCDC 203281 (**1d**), 203282 (**1e**), 203283 (**1f**), 203284 (**1g**). Copies of the data can be obtained on application to CCDC, 12 Union Road, Cambridge CB2 1EZ, UK (email: deposit@ccdc.cam.ac.uk).

JO0206059

(44) Sheldrick G. M. *Acta Crystallogr.* **1990**, *46*, 467−473.

(45) Sheldrick G. M. Program for the Refinement of Crystal Structures. University of Göttingen, Germany, 1993.

(46) *International Tables for X-ray Crystallography*; Kynoch Press: Birmingham, UK, 1974; Vol. IV.